LIFE SCIENCES

Hierarchies in light sensing and dynamic interactions between ocular and extraocular sensory networks in a flatworm

Nishan Shettigar,[1,2] Asawari Joshi,[1] Rimple Dalmeida,[1,2] Rohini Gopalkrishna,[1] Anirudh Chakravarthy,[1] Siddharth Patnaik,[1] Manoj Mathew,[3] Dasaradhi Palakodeti,[1]* Akash Gulyani[1]*

Light sensing has independently evolved multiple times under diverse selective pressures but has been examined only in a handful among the millions of light-responsive organisms. Unsurprisingly, mechanistic insights into how differential light processing can cause distinct behavioral outputs are limited. We show how an organism can achieve complex light processing with a simple "eye" while also having independent but mutually interacting light sensing networks. Although planarian flatworms lack wavelength-specific eye photoreceptors, a 25 nm change in light wavelength is sufficient to completely switch their phototactic behavior. Quantitative photoassays, eye-brain confocal imaging, and RNA interference/knockdown studies reveal that flatworms are able to compare small differences in the amounts of light absorbed at the eyes through a single eye opsin and convert them into binary behavioral outputs. Because planarians can fully regenerate, eye-brain injury-regeneration studies showed that this acute light intensity sensing and processing are layered on simple light detection. Unlike intact worms, partially regenerated animals with eyes can sense light but cannot sense finer gradients. Planarians also show a "reflex-like," eye-independent (extraocular/whole-body) response to low ultraviolet A light, apart from the "processive" eye-brain–mediated (ocular) response. Competition experiments between ocular and extraocular sensory systems reveal dynamic interchanging hierarchies. In intact worms, cerebral ocular response can override the reflex-like extraocular response. However, injury-regeneration again offers a time window wherein both responses coexist, but the dominance of the ocular response is reversed. Overall, we demonstrate acute light intensity–based behavioral switching and two evolutionarily distinct but interacting light sensing networks in a regenerating organism.

INTRODUCTION

The ability to sense and respond to light has evolved more than once and significantly influenced fitness of life forms across nature. Although vision in image-forming vertebrate eyes has been a subject of longstanding fascination, light sensing can evolve in multiple ways. Of the millions of species that respond to light, quantitative studies on the functional and behavioral consequences of light sensing are limited to only a few organisms, especially among invertebrates. However, a better appreciation of the diversity in light-induced behavior may be key to understanding eye evolution (*1*–*3*). It has been reasoned that evolutionary selection is thought to act not just on sensory structures but much more directly and robustly on light-mediated behavior (*1*). Any ability to turn information present in incident light into specific behavioral outputs can lead to a fitness advantage. Therefore, quantitative studies on how different organisms process light and respond to specific light inputs are likely to be extremely valuable.

Light sensing systems have been classified in different ways based on the types of photoreceptors, sensing structures, the neural networks underlying sensory apparatus as well as innovations that enhance specific behavioral functions (*1*–*5*). Simple cup-shaped eyes or eye pits having a pigment cell for directional screening and an array of photoreceptors represent an important eye class (*1*, *2*, *4*). Such eyes, at a minimum, sense the presence and direction of light and may be capable of more advanced functions, classified as low-resolution vision (*1*). This eye type is present in multiple species, spread across the animal kingdom, and likely constitutes an important evolutionary advance (*1*, *3*). However, although some information exists on elements of "low-resolution vision"–like gross spatial mapping (*2*), these eyes are severely understudied. Little is known on how these simple eyes can convert diverse but defined light stimuli into clear behavioral outputs.

Many planarian flatworms have such simple, lensless, cup-shaped eyes broadly classified under low-resolution vision and offer considerable attraction for studying light sensing and behavior (*1*, *4*, *6*). Flatworms, such as *Schmidtea mediterranea* and *Dugesia* species, have prototypic rhabdomeric eyes, with pigment cells and bipolar photoreceptor neurons (PRNs) (fig. S1) (*6*–*10*) with a single opsin reported as the primary photosensor (*11*, *12*). The planarian eye is also a true cerebral eye, with the two eyespots coupled to an early example of a bilobed, brain-like structure (*13*, *14*). Planarians may also be valuable for the study of eye evolution and function because they are members of Lophotrochozoa (*12*, *15*, *16*), one of the most understudied groups in animal phylogeny when compared to other major superphyletic assemblages of the Bilateria, namely, Deuterostomia and Ecdysozoa (*15*, *16*). Apart from this, planarians have remarkable whole-body regeneration potential (*17*, *18*), including the ability to regenerate their brain (dorsal ganglion) and eyes within days (*19*, *20*). Although the process of regeneration has attracted attention (*20*, *21*), much less is known in terms of how regeneration is linked to recovery of sensory function. Therefore, planarians offer unique

[1]Institute for Stem Cell Biology and Regenerative Medicine (inStem), National Centre for Biological Sciences, GKVK Post, Bangalore 560065, India. [2]Shanmugha Arts, Science, Technology and Research Academy (SASTRA) University, Tirumalaisamudram, Thanjavur 613401, India. [3]National Centre for Biological Sciences, GKVK Post, Bangalore 560065, India.
*Corresponding author. Email: akashg@instem.res.in (A.G.); dasaradhip@instem.res.in (D.P.)

opportunities to study how simple eye and light-sensing structures, which are important in the study of eye evolution, can process distinct light stimuli.

Although conceptual understanding of simple eyes is limited, even more elusive is the interplay between different kinds of light responses, having distinct evolutionary histories (*22*, *23*). Apart from eye-based sensing, metazoans can also sense light independent of specific eye structures (*22*, *24*, *25*). Therefore, light responses have also been classified as ocular (eye-mediated) and extraocular (eye-independent) (*25*–*27*). Extraocular or eye-independent light sensing has been reported in many different organisms, including recent examples like *Drosophila* larvae (*27*), *Caenorhabditis elegans* (*28*), and *Platynereis* (*23*). Extraocular photoreception provides a distinct framework in which light can modulate behavior and may also hold important clues on the overall evolution of light sensing in nature. Although eye-based (ocular) (*29*, *30*) and extraocular (*23*, *27*, *28*) light sensing systems have been examined separately, almost nothing is known about relationships and interactions between ocular and extraocular systems in the same organism.

Here, we show that both ocular and extraocular photoresponses are prominent in planarians, with the distinct light responses showing striking hierarchies. We discovered that a simple cup-shaped eye and the associated network are able to resolve acute differences in light stimuli with striking precision and fidelity; even small changes in light input lead to complete switching of light-induced behavior. Further, injury-regeneration offers a way to temporally uncouple gross sensing from the ability to resolve finer differences, offering unprecedented new insights into the buildup of comparative neural processing in eye-brain regeneration. We further show how simple injury-regeneration experiments also allow us to examine, probably for the first time, the dynamic interactions between the two independent (ocular and extraocular) light sensing networks in the same organism.

RESULTS

Behavioral photoswitching in wavelength choice assays

Planarians are known to be light-aversive, with broad sensitivity to visible light (*6*, *10*, *31*, *32*). We confirmed that *S. mediterranea* are negatively phototactic (movement away from light) when illuminated by any single wavelength in the range of 365 to 625 nm (fig. S2, A and C). This demonstrates that planarians are aversive to each of these light wavelengths individually. We then examined planarian behavior in dual-wavelength/binary choice assays. This line of inquiry was significant because planarians have only one known opsin and hence would not be expected to easily discriminate light wavelengths in binary choice assays. In this assay, planarians are simultaneously subjected to two light inputs, of distinct wavelengths and carefully controlled intensities, and worm movement is recorded (Fig. 1A). To our surprise, planarians appear to fully discriminate between light inputs of distinct wavelengths in binary choice assays (Fig. 1, A to C). For instance, if provided a choice between blue (450 nm) and green (545 nm) light of equal intensity, virtually all worms move away from the blue light toward green, with a discrimination index (DI) approaching 1 (0.85 ± 0.022). Although planarians are aversive to each of these light wavelengths individually (fig. S2C), the animals are able to compare the simultaneously provided inputs and make a clear behavioral choice. Similarly, if provided a choice between red light (625 nm) and green light (545 nm), planarians consistently move away from green (Fig. 1B).

We then examined the precision of this apparent discrimination. We found that planarians appear to efficiently differentiate light inputs ~25 nm apart in wavelength (Fig. 1C). DI is consistently high (>0.9) whether the choice assay is performed between 500 and 590 nm, 500 and 545 nm, or 500 and 525 nm, with the worms avoiding 500 nm in each of these cases (Fig. 1C and movies S1 and S2). Further, these precise (~25 nm) behavioral choices are seen across the visible spectrum. Planarians consistently "discriminate" between 450 and 425 nm, 525 and 545 nm, 545 and 590 nm, and 590 and 625 nm light inputs (DI > 0.85; Fig. 1D). Comprehensive binary choice assays showed peak avoidance to be at 450 to 500 nm, with avoidance dropping off on either side of this peak (in choice assays: 425 nm preferred to 450 nm, 525 nm preferred to 500 nm, 545 nm preferred to 525 nm, and so on; Fig. 1D).

Acute light intensity sensing in planarians

Apparent wavelength discrimination by planarians in binary choice assays was surprising. Previous works point to only one major opsin as the primary sensor in the eye PRNs (*11*, *12*, *31*) with no evidence of wavelength-specific photoreceptors. We therefore asked whether the discrimination observed is a consequence of true "wavelength detection" or simply a comparative sensing of individual light wavelengths, all detected by a broad-spectrum photosensor. For this, we first examined whether planarian "wavelength choice" could be reversed through light intensity compensation. This is indeed the case. For instance, although planarians initially preferred the 525 nm over the 500 nm light, increasing the intensity (photon flux = photon fluence rate = number of photons per unit area per unit time) of the 525 nm light input (500 nm was kept constant) led to a neutralization (DI ~ 0) followed by the eventual overturning of choice (Fig. 2A). Significantly, the increase in photon fluence rate required for a reversal in choice scales with increasing difference in wavelength. The photon fluence rate required to reverse the 545/500 nm choice is ~2× the photon fluence rate required to reverse the 525/500 nm choice (Fig. 2A). Upon further examination, we found that it was possible to systematically abrogate choice through light intensity compensation across a wide wavelength range. Increasing the photon fluence rate of the "less-aversive" wavelength in multiple binary choice assays neutralized the clear choice that was observed when equal photon fluence rate was used (Fig. 2A). The generation of a clear "isoluminance point" through light intensity compensation for different wavelength pairs used in binary choice assays suggested that the observed planarian behavior is a form of acute intensity sensing. Phototactic choice is likely being achieved through comparative analysis of the amount of light absorbed at the eye, primarily through a broad-sensing opsin.

Conceptually, spectral differences can be converted into changes in "effective intensities" of light sensed at the eye depending on the absorption spectrum of the photoreceptor. We therefore surmised that the spectral properties of this single opsin photoreceptor should be encoded in the choice behavior. Specifically, the prediction would be that the peak of the absorption spectra would be the most aversive stimuli in binary choice assays and that more light would be required to neutralize choice as the spectral distance from the peak increases. Therefore, we measured the minimum light (number of photons per unit area per unit time, specifically photon fluence rates F_λ) required to neutralize choice for each light wavelength in binary choice assays against a constant 500 nm light input (F_{500}). According to the principle of classical "action" spectroscopy, at the point of choice neutralization,

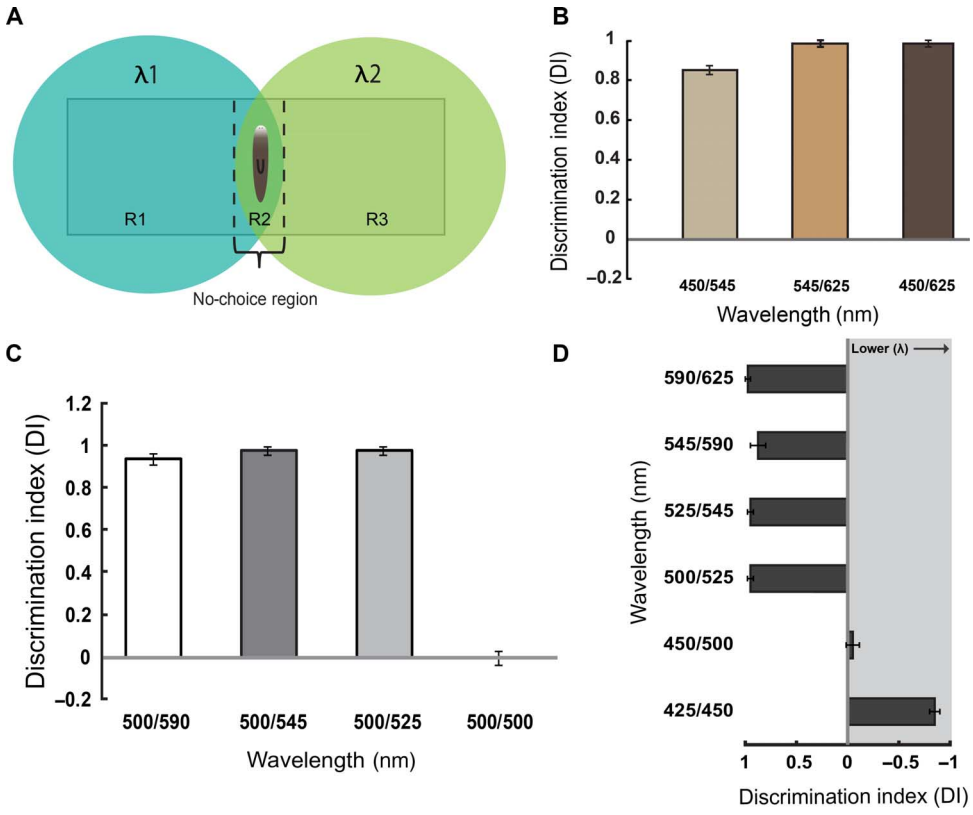

Fig. 1. Planarians show the ability to resolve light inputs of distinct wavelengths. (**A**) Schematic of the binary phototactic choice assay performed. Two simultaneous light inputs of specific wavelengths were provided, and the movement of planarians was measured to determine the choice made—either movement away from λ2 (R1 localization), away from λ1 (R3 localization), or no choice (R2 localization). (**B**) DI shown here for binary choice assays performed with either of the following light pairs: blue and green (450 and 545 nm), green and red (545 and 625 nm), or blue and red (450 and 625 nm). Results of measurements on 10 worms, $n = 6$. Error bars indicate SEM. DI as indicated here and detailed in Materials and Methods. (**C**) Data from binary phototactic choice assay between a 500 nm light input and a second wavelength (525/545/590 nm). DI = (NR3 − NR1)/total number of worms, where NR is the number of worms in a region. A DI value of 1 or −1 indicates a complete aversion or preference for the 500 nm light relative to the second wavelength. A value of 0 indicates no preference. All choice measurements were performed by providing constant light intensity of 316 μW/cm^2 (± 10) for both inputs. Results of measurements on 30 worms, $n = 5$. (**D**) Wavelength discrimination assay performed with wavelengths from 425 to 625 nm with ~25 nm spectral separation. Results of measurements on 10 worms, $n = 4$. (B to D) Error bars indicate SEM.

the photoresponse (proportional to the product of extinction coefficient and number of photons incident) for the two inputs should be identical (*33*) and can be used to build an action spectra. The data showed that across the visible region, the amount of light required to scramble choice gradually increases away from 450 to 500 nm (peak aversion). Further, the wavelength plot of the photon fluence ratios (F_{500}/F_{λ}) at choice neutralization yielded a behavioral action profile (see Fig. 2B and Materials and Methods) that resembled the absorption spectra of a single photoreceptor. This action response curve could be matched for a preliminary comparison to the predicted absorption spectra of the "alpha band" of a single hypothetical opsin (Fig. 2B), based on Govardovskii's template (*34*).

It is remarkable that the measurement of light intensity modulation in wavelength choice assays could yield a response curve or behavioral "action spectrum." In addition, the unimodal shape of this choice neutralization response profile strongly supports the model of planarians using a single primary photoreceptor for eye-based sensing. To address this further, we then examined the spatial distribution of the primary opsin in the planarian eye. Previous works show that light intensity–independent, true "color" vision requires multiple opsin pigments and multiple opsins tend to show spatial segregation in PRNs in eye structures (*35*–*38*). Fluorescence in situ hybridization (FISH) imaging of the Smed eye opsin mRNA shows that the primary opsin likely expresses throughout the eye (Fig. 3, A and B). Costaining with labeled anti-arrestin (VC-1) antibody allowed us to mark every single PRN, and imaging with confocal microscopy revealed that every single PRN does express the primary eye opsin (Fig. 3, B and C, and movies S3 and S4). These data strongly suggest that all PRNs likely use the same primary opsin photoreceptor for sensing. We then performed RNA interference (RNAi)–based knockdown of the primary eye opsin gene (*11*, *12*, *39*). Knockdown of this single opsin mRNA attenuates light sensing response across the visible spectrum in planarians (fig. S3), providing further evidence that acute discrimination shown by planarians in binary choice assays does not depend on wavelength-specific photoreceptors.

Hierarchical light processing revealed through regeneration

Our data so far suggest that the organisms are able to resolve small differences in effective intensities of light sensed at the eye and convert these differences into binary behavioral outputs. This behavioral fidelity points to highly efficient post-sensory comparative processing mediated through the visual neural network. To address this, we

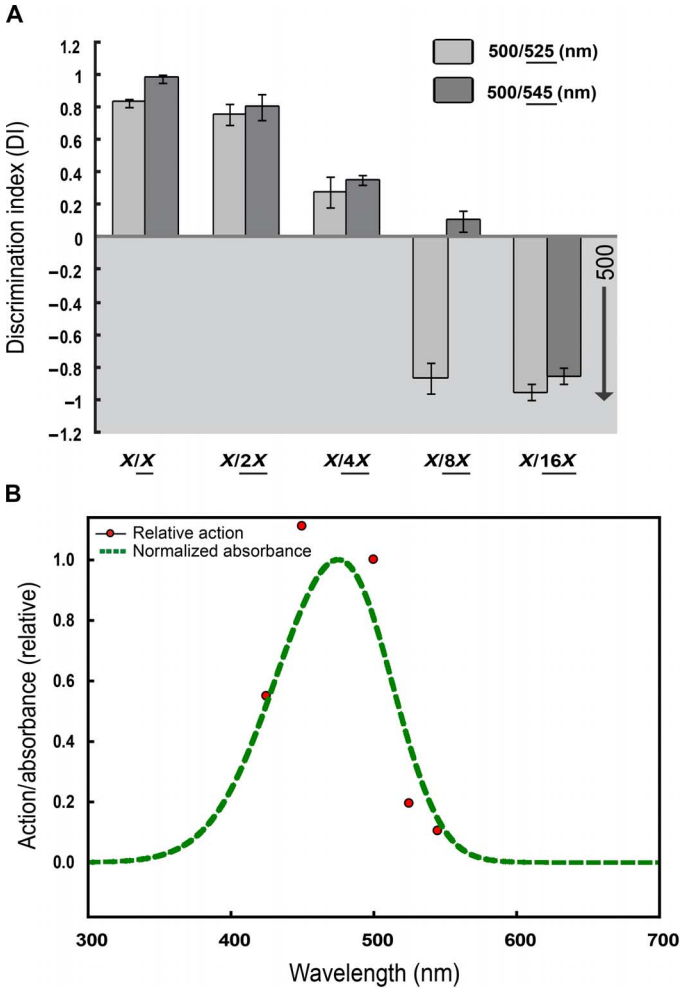

Fig. 2. Light intensity–based neutralization of wavelength choice yields an "action" spectrum that resembles an opsin absorption curve. (**A**) Overturning of choice through light intensity dosage. Binary choice experiments were initially performed with equal amounts of photon flux (photon fluence rate – X = 1.59 × 10^{14}/s per cm^2). Photon flux of less-aversive input was then increased as indicated. Results of measurements on 10 worms, n = 4. (**B**) Putative action spectrum determined by measuring the amount of light required for choice neutralization in binary choice assays with respect to 500 nm (near peak). Plotted here is a ratio of photon fluence rates (F_{500}/F_λ) versus wavelength (λ) in nanometers at the point of choice neutralization. The photon fluence rate at 500 nm was kept constant (1.59 × 10^{14}/s per cm^2), whereas the amount of light for other wavelengths (F_λ) was modulated to determine minimum light required for choice neutralization in binary assays. For all wavelengths other than 450 nm, an increase in photon fluence rate was required to neutralize choice with 500 nm. Results of measurements on 10 worms, n = 4. This obtained profile was matched with the predicted spectrum of the alpha band of an opsin with a λ_{max} of 475 nm, based on Govardovskii's template (*34*).

exploited the ability of planarians to regenerate their eye and the brain after amputation. Specifically, we examined the return of phototactic ability, including fine intensity discrimination (assayed through wavelength choice) as a function of regeneration. After amputation, planarians show head regeneration approximately over a week (*40*). Eye spots (pigmentation) become visible after ~4 days (Fig. 4A). If we examine the return of single-input light sensing and response in a light-dark assay, planarians show a robust negative phototactic response by ~5 days after amputation (fig. S4); this response is stable thereon. Remarkably, however, in binary choice assays at days 5 and 6 after amputation, planarians do not show clear phototactic choices seen with intact worms. Consistent choice behavior with multiple, closely spaced inputs is seen significantly later in regeneration (Fig. 4B).

Regeneration experiments show a hierarchy in light sensing and processing wherein the acute "effective intensity" discrimination is layered on a gross ability of the worms to detect light. In regeneration, by day 5 after amputation, a basic eye structure is established (*20*), and the visual network is able to signal to the locomotor system, leading to gross light-dark phototaxis (Fig. 4B). However, at this stage, the worms do not show acute intensity discrimination. The return of this finer discrimination, over subsequent days, likely requires further rebuilding in the visual network such that comparative processing of two very similar inputs can be accomplished. Imaging of the planarian neural network shows that significant changes occur in the regenerating planarian brain at specific time points that correlate with functional recovery of light sensing. Laser scanning confocal immunofluorescence microscopy with a synaptic marker reveals that by day 5 after amputation, a basic framework of the regenerated ventral nerve cord, cephalic ganglion (brain), and the eye gets assembled, consistent with behavior. However, there is a substantial enrichment and enlargement of the planarian cephalic ganglia between days 5 and 7 after amputation. This can be seen from representative imaging planes (Fig. 4D) and analysis of all z-stacks corresponding to the two cephalic lobes of the dorsal ganglion (movies S5 to S9) during regeneration. This progressive enrichment of neural network was further tested through a careful examination of functional recovery. Figure 4C shows that although coarse "discrimination" is restored to an extent by day 6 (90 nm differences in λ; DI = 0.67 ± 0.014), the ability to do finer discrimination is significantly delayed. An ability to discriminate between inputs 25 nm apart is only seen 12 days after head removal (Fig. 4C). These data showing progressive enhancement of behavioral complexity with time provide a significant new insight that "functionally relevant regeneration" continues much after gross repair of organ systems has occurred.

Eye-independent, directional light avoidance in planarians

Planarians are highly light-aversive and show complex light discrimination through their cerebral eyes. We then examined whether planarians have other modes of light sensing, including eye-independent modes. For this, we observed the response of head-removed (amputated) planarians to light. We found that *S. mediterranea* showed a striking extraocular, whole-body response to long-wavelength ultraviolet (UV) light (Fig. 5A and movie S10). Although there are early reports suggesting whole-body light sensing in planarians (*10*, *32*), we quantitatively examined this sensing in the context of our new findings. Movie S10 shows that although freshly decapitated (head-removed) planarians show no significant movement in "visible/white" light, illumination with long-wavelength UV light (360 to 400 nm) leads to robust movement of the headless worm away from light. This movement of headless worms, in response to UV, is reminiscent of motion exhibited by intact worms. To test the precise wavelength sensitivity of this extraocular photoavoidance, we examined the response of head-amputated planarians when stimulated with light wavelengths ranging from 365 to 625 nm (fig. S5). Head-amputated worms responded primarily to wavelength from ~365 to ~395 nm in photoavoidance assays, with significantly reduced or no response at 405 nm and beyond. Modified photoavoidance assays showed that

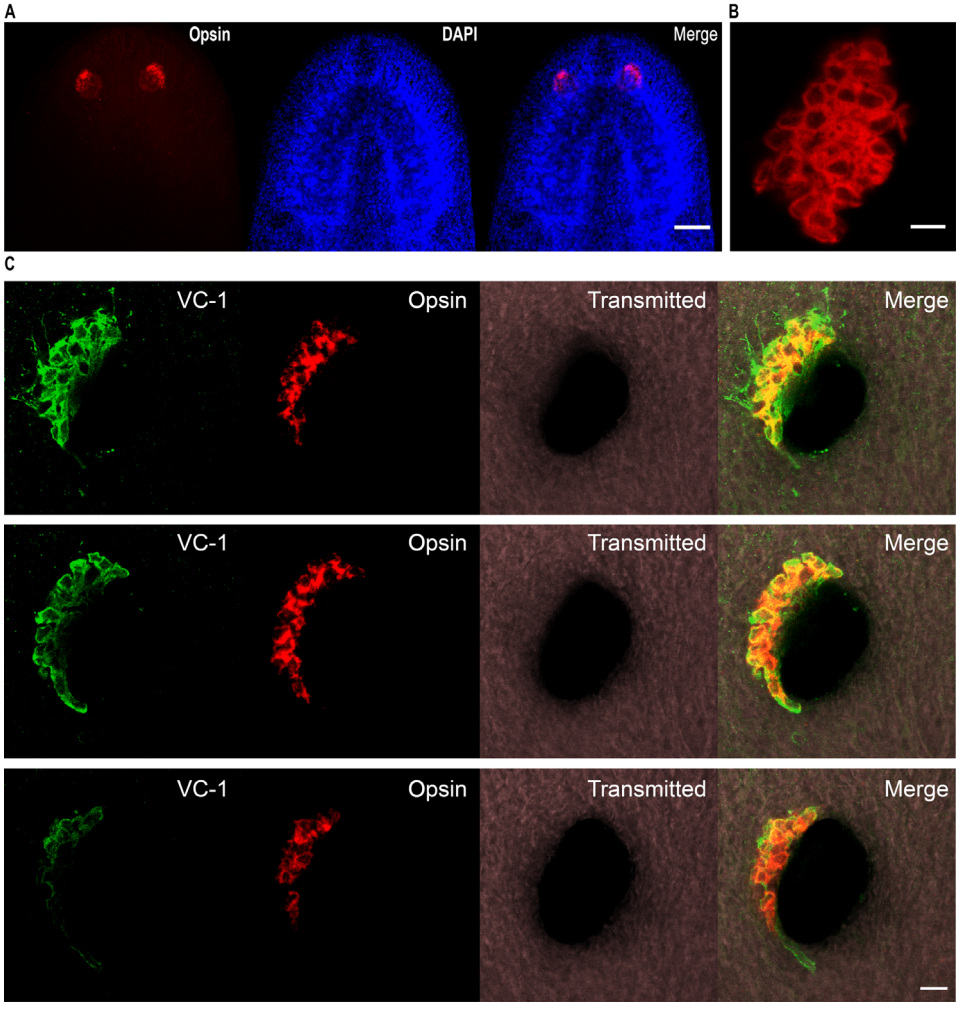

Fig. 3. Smed eye opsin expression is restricted only to eye and is expressed in all PRNs. (**A**) Confocal *Z*-projected image of FISH of Smed eye opsin (red) and 4′,6-diamidino-2-phenylindole (DAPI) (blue) highlighting cephalic ganglion in the worms. Scale bar, 100 μm. (**B**) Representative stack of laser scanning confocal image of Smed eye opsin (red) FISH showing individual photoreceptor cells. Scale bar, 10 μm. (**C**) VC-1 (green) antibody staining along with Smed eye opsin FISH (red) merged with the transmitted image showing eye pigmentation. Dorsal, middle, and ventral stacks (top to bottom) showing coexpression of arrestin and Smed eye opsin. Scale bars, 10 μm.

the time taken for movement of head-removed pieces out of a light spot was significantly greater for 405 nm compared to inputs in the 365 to 385 nm region (fig. S6), showing a clear wavelength-dependent attenuation of this photoavoidance behavior. There was little or no response at longer wavelengths across the visible spectrum. This showed that extraocular photoresponse was reliant on a sensory network distinct from the cerebral eye–based system, with distinctive photoreceptor molecules (see Discussion). Asymmetric and localized illumination of head-removed worms with 385 nm light spots (movie S11) further confirmed that the extraocular photoresponse to long UV is directional. In these assays, amputated pieces show movement/turning away from the direction of light.

Dynamic interplay among ocular and extraocular sensing networks

Planarians appear to have separate ocular and extraocular sensing systems. This provides a unique opportunity to explore the relationship and contrasts between these distinct sensing modalities in a single organism. To pursue this, we first illuminated worms simultaneously with long UV (395 nm) and "visible" light (500 nm) and measured their choice. Remarkably, in these dual-wavelength choice assays, planarians show movement away from the 500 nm light, "preferring" the 395 nm light of the same intensity (DI = 0.8 ± 0.05). Although both long UV and visible light are aversive signals, if provided simultaneously, the worms make a clear choice, showing greater aversion to visible light (Fig. 5C). This is noteworthy. Planarians sense visible light through their cerebral eye. On the other hand, UV light sensing (extraocular) is dispersed throughout the planarian body. In a competition experiment, the aversive response through the cerebral eye appears to be dominant. This hierarchy is consistent with the extraocular (whole-body) response being a reflex-like response, whereas the ocular response is a brain-mediated processive response. To test this further, we compared how the extraocular and the ocular responses scale with light dosage. Extraocular phototaxis shows clear dose dependence—the time taken for a headless worm to move out of a circular spot, in response to UV, progressively reduces with an increase in light intensity followed by saturation (Fig. 5B). In contrast, for ocular photoreception, the total phototactic time is

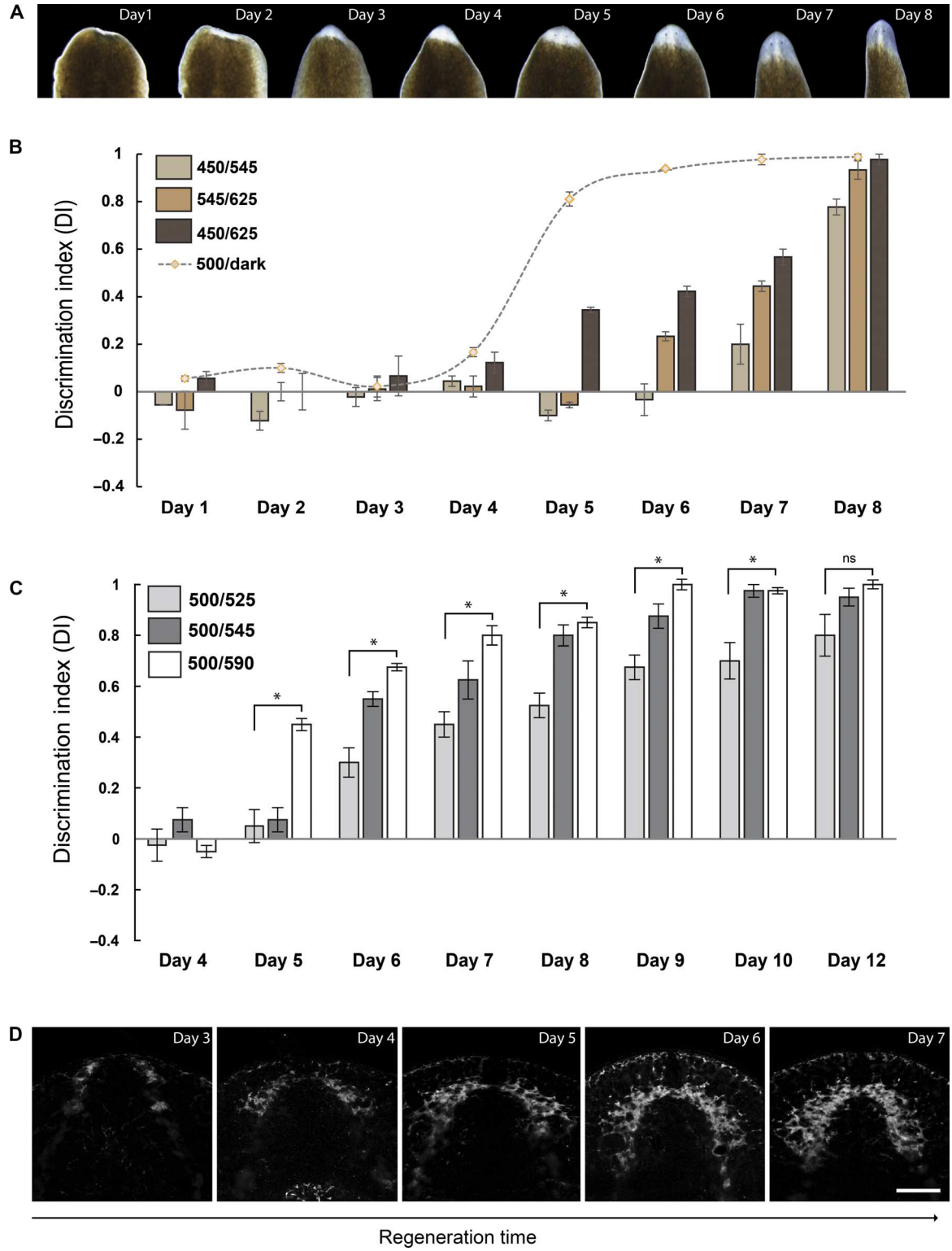

Fig. 4. Mapping recovery of planarian phototactic abilities during regeneration. (**A**) Images showing head regeneration in *S. mediterranea* from days 1 to 8. (**B**) Wavelength discrimination assay performed on regenerating worms, with blue and green (450 and 545 nm), green and red (545 and 625 nm), and blue and red (450 and 625 nm) light inputs. Measurements with 10 worms each, $n = 6$. Gray dashed line indicates the return of single-wavelength input (500 nm) negative phototactic ability (see also fig. S4). (**C**) Comparative recovery of finer wavelength discrimination ability in regeneration. Binary choice assays with the light wavelength pairs 500/590, 500/545, and 500/590 nm over regeneration. Measurements on 10 worms each, $n = 4$. (B and C) Error bars indicate SEM. ns, not significant. (**D**) Immunostaining of planarian cephalic ganglion using SYNORF1 antibody during the course of regeneration from days 3 to 7. Scale bar, 100 μm. *$P < 0.05$.

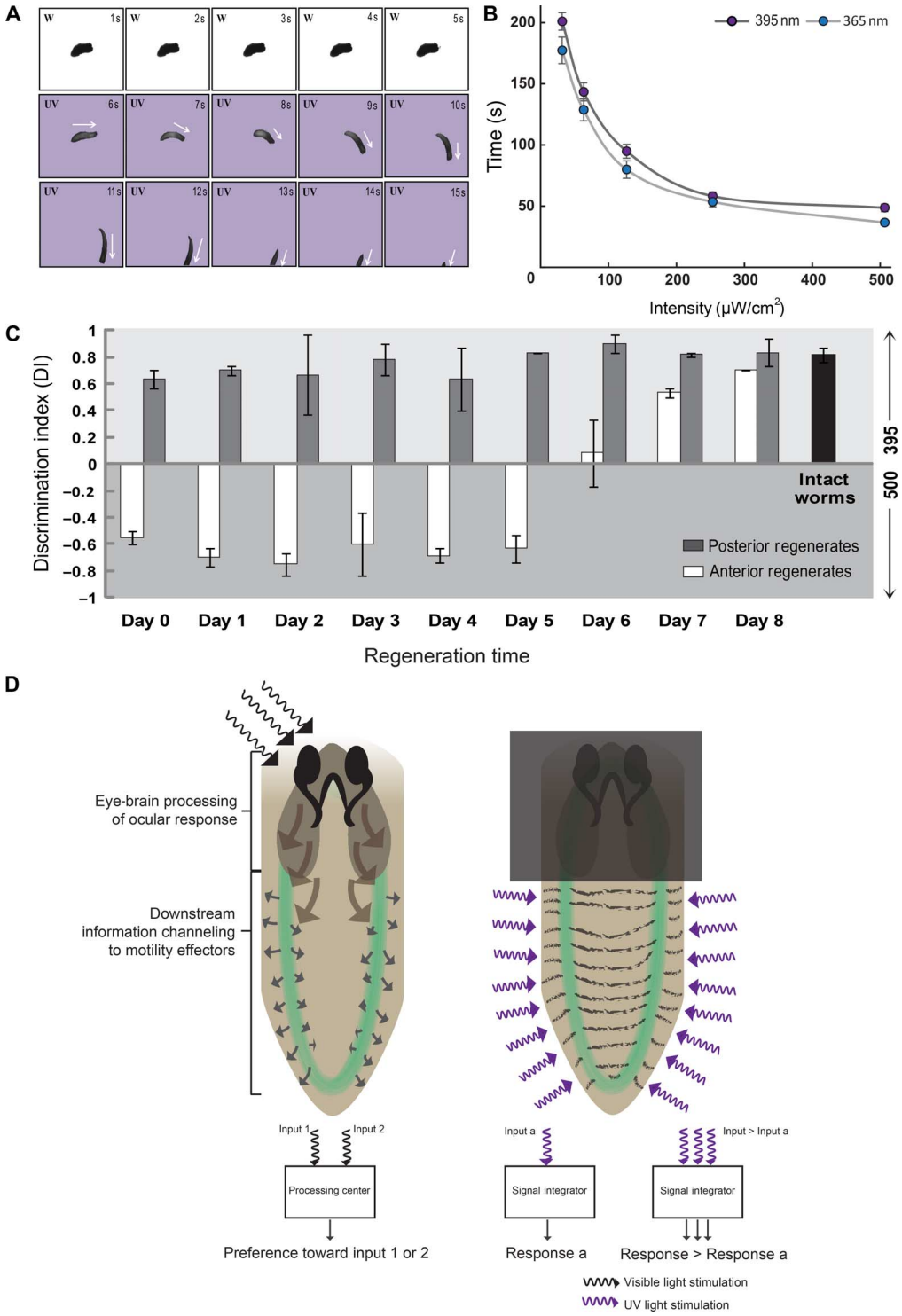

Fig. 5. Planarian extraocular photoresponse and hierarchical relationship with ocular light response. (**A**) Snapshots of amputated worms showing light avoidance under UV light (350 to 400 nm) and no light avoidance under white light (W). (**B**) Dose dependence of extraocular photoresponse. Time taken for a headless tail piece (24 hours after amputation) to move out of a circular spot of the 365 or 395 nm light (n = 30; see details in the Supplementary Materials). (**C**) Interplay between ocular and extraocular light response in regeneration. DI for choice assays between 395 and 500 nm light in anterior and posterior regenerates during time course of regeneration. DI for intact worms is also shown (right). Error bars indicate SEM. (**D**) Conceptual model indicates multiple facets and diversity in planarian light sensing. The ocular response mediated through the cerebral eye is a "processive" response, including the capacity for wavelength discrimination. This discrimination appears dependent on comparative processing of input signals through the visual network. On the other hand, the extraocular response to UV light appears to be a more rudimentary response with the ventral nerve cord and peripheral network likely functioning as an integrator, collecting and mediating a whole-body response leading to coordinated phototaxis. Both ocular and extraocular light sensing modalities engage the same motor machinery.

insensitive to dosage (fig. S7). Because extraocular response involves whole-body sensing, the speed of response appears to depend on the total light sensed across the worm. However, in contrast, because the ocular response appears to be subject to processing by the neural network, the total time required for movement is insensitive to light dosage (Fig. 5D). In addition, head-removed worms fail to show any spectral choice (fig. S8) unlike intact worms that show processing-based discrimination in binary choice assays.

We then examined this hierarchical relationship between the brain-mediated ocular and the whole-body extraocular responses during eye-brain regeneration. Figure 5C shows aversive choice between UV light (395 nm) and visible light (500 nm) plotted as a function of time after head removal. As expected, freshly cut decapitated worms subjected to UV/visible choice show movement away from UV. Head-removed, eyeless worms cannot sense visible light; hence, UV response dominates. Expectedly, this choice pattern is maintained until 4 days after decapitation—there is no functional eye or any response to visible light (fig. S4). However, by day 5 after injury, planarians regenerate a "functional" eye and a phototactic response to visible light (fig. S4). Therefore, by day 5, the eye-brain is functionally connected to the locomotor systems, and planarians respond to stimuli sensed at the eye. However, at this stage (day 5), the extraocular response retains its dominance over the nascent cerebral response in choice assays, wherein regenerating worms still show movement away from UV (toward visible light) (Fig. 5C). This is opposite to the behavior with intact worms. Remarkably, this result implies that regenerating worms that have sufficiently regenerated a functional eye and brain capable of phototaxis behave similarly to headless, tail pieces in ocular-extraocular choice experiments. Subsequently, there is a transition about day 7 after decapitation, wherein the choice is reversed. By day 7 after injury, the regenerating planarians resemble intact worms, wherein the ocular, brain-mediated response is stronger and can override the extraocular response (Fig. 5C). These data reveal the remarkable plasticity in the cross-talk between the two distinct responses—ocular and extraocular—mediated by two independent but interacting neural networks in the same organism.

DISCUSSION

Planarian flatworms are highly light-aversive organisms often found in dark, aqueous environments shielded from direct light (*41*). Although reports of photoavoidance responses to visible and UV light in planarians exist, a conceptual and mechanistic understanding of light sensing in these organisms is limited. How do planarian flatworms respond to light? What are the different ways in which planarians, with prototypic "simple" eyes, process information encoded in light stimuli? Several of these questions have remained open. Our data show that planarians have at least two independent light responses, ocular and extraocular, anchored in distinct sensory networks. The ocular response to visible light is mediated through the cerebral eye (fig. S1A), whereas the extraocular response is a whole-body response, with head-removed planarians able to respond to even small doses of long UV light (Fig. 5B). Our work uncovers new light sensing and processing modalities while also showing how independent light sensing systems can interact.

In examining the ocular (eye-based) sensing, we made new discoveries. In binary wavelength choice assays, planarians show consistent phototactic choice with exceptional fidelity throughout the visible spectrum. Even a 25 nm change in wavelength inputs is sufficient to fully switch the phototactic behavior. Although differential single-input photophobic responses have been reported (*10*), this is the first report on how planarians or similar organisms can acutely sense closely spaced spectral stimuli and convert them into these distinct behavioral outputs. Conventionally, specific photoreceptors are required for true wavelength detection (*35*–*37*). However, planarians reportedly have only a single, broad-sensing opsin photoreceptor in the eye (*11*, *31*). Our data show that this single opsin is expressed throughout the eye, within every individual PRN (Fig. 3, B and C, and movies S3 and S4). In organisms with wavelength-specific opsins, these tend to be spatially confined to subsets of PRNs in the eye, allowing for true wavelength detection (*38*). Besides, our RNAi knockdown of the primary eye opsin leads to reduced photosensitivity across the spectral range (fig. S3). These data strongly suggest a single opsin photoreceptor in the eye.

So how do the animals respond to small changes in light wavelengths without specific photoreceptors? Broad-sensing photoreceptors should be refractory to small spectral changes. Photoreceptors are extremely sensitive "photon counters," but once an opsin is photoexcited by one of two spectrally similar stimuli, the wavelength information is "lost" (*35*). The phototactic choice seen in our assays is not true "wavelength discrimination" but a manifestation of an acute intensity sensing using a single photosensor. We find that simple modulation of light intensities is sufficient to neutralize and even reverse wavelength choice (Fig. 2A). Further, measurements of intensities (photon fluence rate) required to neutralize wavelength choice (behavior) yield a putative action spectrum, demonstrating the robustness of response (Fig. 2B). Although this unimodal action spectrum is consistent with a single eye opsin, further microspectroscopic analysis would be required to precisely define the absorption profile of the eye.

We propose that worms sense small wavelength changes by comparing the effective intensity of light inputs sensed at the eye. In the simplest scenario, the signal sensed would scale with the actual absorption of light by the eye. For any given wavelength, the light absorbed would be a function of the intensity of incident light and extinction coefficient of the photoreceptors. Given two equal intensity (photon fluence rate) light inputs of different wavelengths (even with a single opsin photoreceptor type), there will be differences in the amount of light sensed at the eye, reflecting the intrinsic absorption spectrum of the opsin. Remarkably, when illuminated with closely spaced spectral inputs, the animals are able to convert small differences in effective intensities into virtually binary behavioral choices. Differences in effective intensities likely lead to changes in aggregate PRN response and signaling to a putative downstream processing center. The networks are able to parse these differences in effective intensities through comparative processing, leading to phototactic choice. This choice can also be described as acute gradient sensing. Gradient sensing is seen in other organisms, such as *Platynereis* (*42*) and *Drosophila* larvae (*43*). Although planarians appear too acutely sensitive, this ability to sense light gradients likely represents a widespread evolutionary advance. Further work would be required using RNAi and imaging methods to look for mechanistic and structural underpinnings of acute gradient sensing.

In contrast to this "processive" cerebral eye light sensing, the high-sensitivity planarian whole-body extraocular photoresponse appears to be a reflex-like response (Fig. 5, B and D, and fig. S6). Unlike with ocular response, the extraocular response times scale strongly with light intensity; also, wavelength choice patterns, seen with eye-mediated sensing, are absent. The extraocular response network appears to integrate

whole-body sensing events, finally leading to directional phototaxis (Fig. 5, A and D). Even the photoreceptor(s) mediating the extraocular response is distinct from the eye opsin, with different spectral ranges. High sensitivity to long UV (proxy for filtered sunlight) is consistent with the environmental niche of many planarians. Being highly light-aversive, a whole-body response may be beneficial. Many planarians can also propagate through fission (*41*, *44*). A robust, phototactic extraocular response would allow newly fissioned, vulnerable tail pieces to avoid direct or bright light.

How is UV-A sensed and processed? Opsins are some of the most widely expressed light sensing proteins in the animal kingdom (*26*). Extraocular sensing using opsins has been seen in several organisms spread across different phyla (*26*). However, novel photoreceptors cannot be discounted. For instance, *Drosophila* larvae (*27*) and *C. elegans* (*28*) reportedly use unconventional light receptors resembling gustatory receptors for extraocular sensing (named Gr28b in *Drosophila* and LITE-1 in *C. elegans*). Reports also suggest that transient receptor potential ankyrin 1 (TRPA1) channels may also respond to UV light (*27*, *45*). To list the possible extraocular photoreceptor molecules in *Schmidtea*, we conducted a preliminary investigation using bioinformatics. A pipeline designed to look for opsin-like proteins in the existing planarian transcriptome yields six candidates (fig. S9), excluding the previously identified eye opsin. We were unable to find any homologs for LITE-1 and Gr28b in our analysis, but found one TRP channel candidate when comparing *Schmidtea* TRP channel homologs with UV-sensitive human and *Drosophila* TRPA1 channels (fig. S10). Our preliminary analysis, based on molecules that have been implicated in extraocular photoreception in other organisms (opsins, gustatory receptor–like, and TRP channels), yields some candidate photoreceptor(s). Further work would be required to identify the light receptor(s).

Planarian tails show coordinated movement away from UV, suggesting an independent neuronal signaling–dependent locomotor response. Where does the photosensing occur? In some organisms showing extraocular sensing, photoreceptor molecules have been reported in neurons (*23*, *27*, *28*). Classical nervous system studies and immunostaining have showed the existence of subepidermal nerve plexus in planarians (*46*–*48*). Therefore, it is conceivable that light sensing molecules present in these neurons lead to extraocular response. There have been reports on ectopic eyes present in polychaetes (*49*); however, there is little or no information on these photoreceptive structures in planarians. Investigating the structural and functional underpinnings of this high-sensitivity extraocular response would be fascinating.

Because planarians show full eye-brain regeneration after injury, it is possible to address the nature of light sensing and processing in unprecedented ways. Examining functional recovery of light sensing revealed a hierarchical, multilayered sensing paradigm. For eye-mediated light sensing, our data from wavelength choice experiments performed over eye-brain regeneration showed how gross sensing could be temporally delineated from finer sensing (Fig. 4A). There is a period of time when regenerating worms (unlike intact worms) can sense light but cannot show clear behavioral choices in binary wavelength assays. Thus, the effective intensity–based acute gradient sensing is layered on a basic ability to detect light, with a progressive buildup of sensing and processing capacity. We show that the ability to discriminate closely spaced inputs (~25 nm changes) recovers significantly later than crude discrimination abilities (Fig. 4C). This reveals that functional recovery continues much after gross regeneration of the eye-brain structures is complete. Full functional recovery likely requires fine-tuning of sensing and processing capabilities, involving pruning and patterning of the neural networks. Regeneration data support our model that acute sensing likely involves significant post-sensory comparative processing. Confocal imaging of planarian brain using a synaptic marker over regeneration is consistent with progressive buildup of neural capacity (Fig. 4D). Although gross regeneration of basic brain structures appears to be complete by about day 5 after decapitation, significant enrichment of synaptic density coincides with the recovery of acute sensing and processing abilities. Light sensing assays established here may provide a new way to functionally "map" neural regeneration (Fig. 6A).

Existence of two independent light sensing networks in planarians, along with eye-brain regeneration capacity, again allows unique lines of inquiry. For intact worms, in competition experiments, the cerebral ocular response can override the reflex-like extraocular response, setting up a baseline hierarchy among the responses (Fig. 5C). Ocular-extraocular choice experiments during regeneration reveal remarkable plasticity in these hierarchies. During eye-brain regeneration, there is a period of ~36 hours wherein both the extraocular and ocular responses "functionally" coexist, but the developing eye-brain axis is unable to override the reflex-like extraocular response (Figs. 5C and 6B). Thereafter, following a clear transition, the dominance of the ocular or brain-mediated response is reestablished (Figs. 5C and 6B). If the extraocular response is a more rudimentary, ancient response predating the eye and a processive brain, then does regeneration coincidently mimic aspects of evolutionary trajectories?

Ocular-extraocular choice experiments over regeneration also provide new insights into how the eye-brain network interacts with the whole-body light sensing network (Figs. 5C and 6A). A headless worm can undergo locomotion in response to UV. By about day 5 in regeneration (after head removal), a cerebral eye and a minimal brain are established, which link to the ventral nerve cord, whole-body nervous system, and the locomotion machinery. This link of the visual network to the locomotor network is sufficient to generate movement in response to light. However, it appears that the signaling flux from the cerebral eye and brain at this point is still insufficient to override the extraocular or reflex-type response anchored in the whole-body neural network. After day 7, we propose that this signal from the eye-brain to the whole-body system strengthens, allowing overriding of the extraocular response (Fig. 6B). Appearance of a threshold wherein brain-mediated response begins to dominate a whole-body response has implications for how the eye and the cephalic ganglion regenerate and how connectivity between two distinct neural networks, the cephalic ganglion and the ventral nerve cord in this case, is established and fine-tuned during regeneration. To our knowledge, this may be the first report of its kind, describing such clear and dynamically interchanging hierarchies between two distinct light sensory systems, all revealed through relatively simple phototactic choice assays performed over regeneration.

In summary, this study significantly affects our fundamental understanding of light sensing responses. Our work highlights the remarkable diversity and plasticity in light sensing and processing that remain unexplored in nature. Because planarians have eye structures and neural networks that appear simple yet similar to those observed in other animals, these acute and distinct light sensing and processing abilities may be more widespread in nature. This work also sets the stage for a comprehensive examination of light-induced behavior in flatworms wherein new questions based on comparative visual processing and regeneration of neural networks can now be addressed. Our

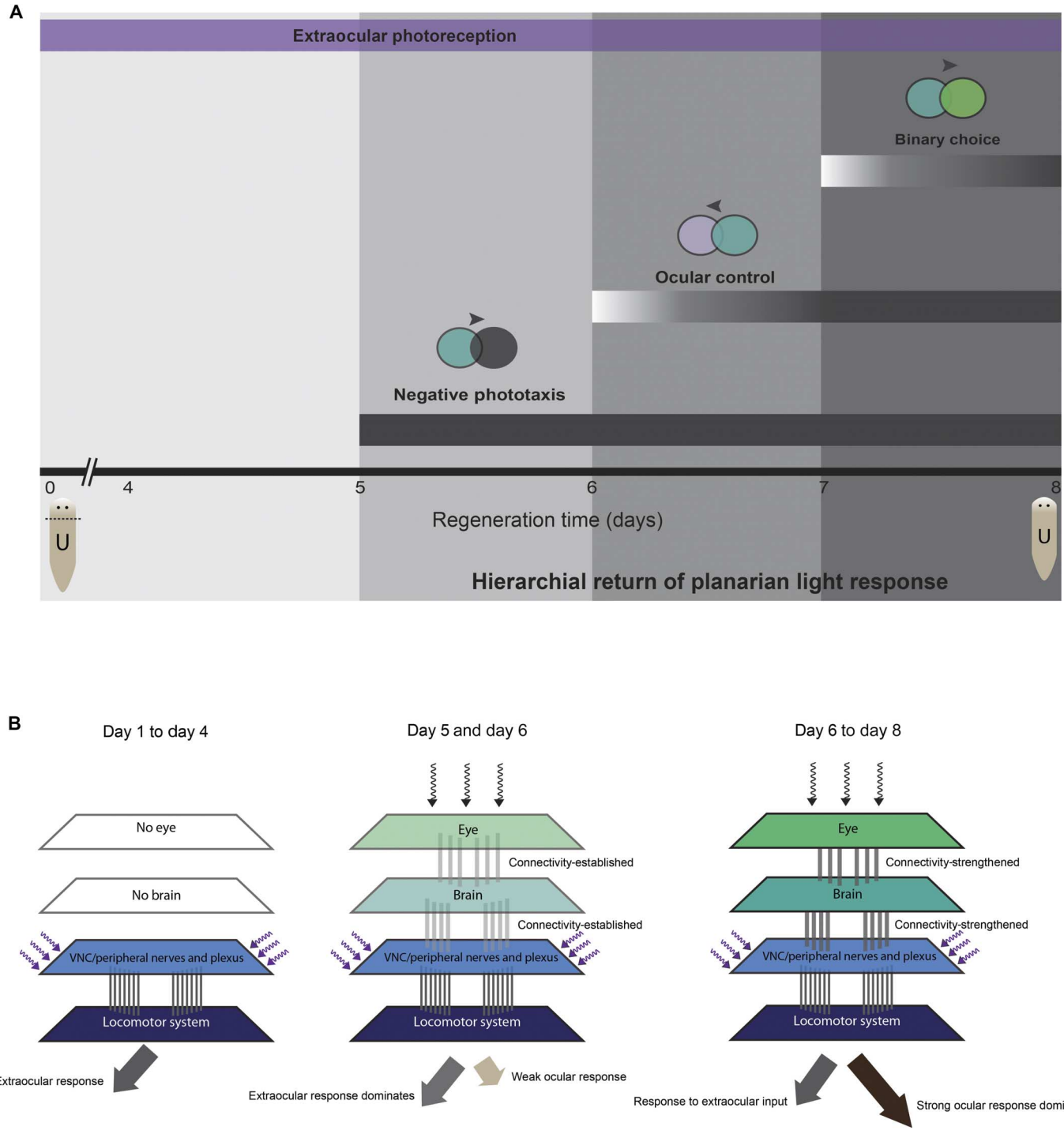

Fig. 6. Hierarchical light sensing and processing in planarians revealed through recovery of function with regeneration. (**A**) Schematic showing a timeline of return of different phototactic abilities during head regeneration in *S. mediterranea*. By day 5 after amputation, worms sense light but have no ability to finer intensity discrimination (assayed through wavelength choice), which is acquired gradually significantly later. See (B) for ocular control. (**B**) Model for hierarchical relationship between networks regulating ocular and extraocular sensing, including switching during regeneration. During days 1 to 4 after amputation, worms show only extraocular response anchored in ventral nerve cord (VNC) and peripheral neurons. By about day 5, ocular response recovers in worms, but signaling flux from cerebral visual networks is unable to override signals resulting from extraocular photosensing. Ocular and extraocular photosensing coexist, but extraocular sensing is dominant in competition assays. Day 7 onward, flux from visual network strengthens, allowing the ocular response to be dominant, as in intact worms. Black arrow indicates visible light input, whereas violet arrow indicates long UV light input.

results demonstrating the interplay between ocular and extraocular light sensing networks are likely without precedent and reveal the rich and multilayered light responses in planarians that can now be examined further.

MATERIALS AND METHODS

Light source and measurements

Wavelength-specific light-emitting diode (LED) light sources were procured from Roithner Lasertechnik. The specific LEDs used were 365 nm (XSL-365-5E), 395 nm (RLS-UV395), 425 nm (LED425-6-30), 450 nm (LED450-01), 500 nm (LED500-10-30), 525 nm (LED525-01), 545 nm (LED545-04), 590 nm (LED590-03), and 625 nm (B5B-435-TL). Each LED is referred by its peak wavelength in the study. A suitable LED circuit along with a regulatable power source to drive the LEDs was assembled. This allowed precise control of LED light intensities. Custom-designed OptoLED illumination system (Cairn Research) (fig. S11) was also used for extraocular-mediated behavior experiments. Light power measurements were made using Newport power meter 1918-R and 918D detector. Light measurements for all initial binary choice experiments were made at microwatt per square centimeter ($\mu W/cm^2$; intensity). All behavior experiments were performed with approximate measurement error of ±10 μW. For the experiments involving neutralization (and overturning) of wavelength choice, the unit of light measurement and intensity was photon flux or photon fluence rate (number of photons per unit time per unit area). This was done to ensure consistency with the theory of action spectroscopy and to build a wavelength-dependent response function using light intensity required for neutralization of choice behavior. The stability of the signal was checked for the duration of the experiment in all cases.

Planarian maintenance

S. mediterranea was maintained at standard laboratory conditions (*50*). Worms were fed beef liver extract once in 3 days. Worms were starved for at least 2 days before the start of any experiment. In addition, behavior experiments were performed in a dark room maintained at 20°C.

Planarian negative phototaxis (single-input sensing)

Earlier work shows that planarians respond broadly to visible light, with subtle differences in response to colors (*10*). Using single-wavelength phototaxis assays, we confirmed that planarians (*S. mediterranea*) are negatively phototactic to visible light (fig. S2C). Sensitivity attenuates at wavelengths ≥625 nm (fig. S2C). The setup for the single-input, light-dark phototaxis has been illustrated in figs. S2A and S11. Planarians were starved for at least 2 days for all phototaxis experimentation on intact or regenerating worms. Light-dark phototaxis assays with planarians were performed on a glass slide (75 mm × 25 mm × 1.25 mm). About 5 ml of medium was added to the slide, and a single planarian was placed in the center region (R2, 10 mm wide; fig. S2A) using a Pasteur pipette. Following this, LED light was turned on (all intensities were set to ~316 $\mu W/cm^2$) such that illumination was spatially polarized creating a lit (R1) and a relatively dark zone (R3). After 2 min, the region (fig. S2A) in which the planarian is present is determined. This is repeated for several worms, and a DI is calculated. DI was calculated by using the formula: DI = (NR3 − NR1)/total *N* (where NR is the number of worms in a region, and *N* is the number of worms). A DI value of 1 or −1 indicates a complete aversion or preference for the provided wavelength of light, respectively. A value of 0 indicates no preference. Phototaxis during regeneration was also performed as described above, except that the position of the worm was determined after 3 min.

Wavelength discrimination choice assays

All planarian choice assays were performed according to the schematic shown in Fig. 1A. LED lights were used as above. For all binary wavelength choice assays with equal intensities, two equal-intensity light inputs at a constant light intensity of 316 (±10) $\mu W/cm^2$ were used. Similar to the single-input phototactic assay described above, each worm was placed in the center region and allowed to make a choice with a cutoff time of 2 min. Outcomes can be movement to region 1, region 2, or no choice. Similarly, binary choice experiments were performed during regeneration, and the position of the worm (for calculation of DI) was determined after 3 min.

For experiments testing overturning of wavelength choice through light intensity dosage (Fig. 2A), the initial effective photon fluence rate (number of photons per unit time per unit area) was set at *X* (1.59×10^{14}/s per cm^2) (for both wavelengths). Increasing dosage of the less-aversive input was provided as 2*X*, 4*X*, or 8*X* as indicated in the figures. For building a behavioral response profile to address intensity-based wavelength choice neutralization (Fig. 2B), we measured the increase in photons (photon fluence rate) required to neutralize (randomize) choice relative to the 500 nm light at *X* photon fluence rate (1.59×10^{14}/s per cm^2). Choice neutralization experiments were performed with 425, 450, 525, and 545 nm as second wavelengths. According to the principle of a classical action spectroscopy, at the point of choice neutralization, the photoresponse (*R*; proportional to the product of extinction coefficient and number of photons incident) for the two inputs should be identical (*33*) and can be used to build an action spectrum

$$R_{500} = R_{\lambda} \Rightarrow \varepsilon_{500} : \varepsilon_{\lambda} = 1/F_{500} : 1/F_{\lambda}$$

(*33*) where *R* is the photoresponse, ε is the extinction coefficient, and *F* is the photon fluence rate (number of photons per unit time per unit area). Therefore, the plot of ratio of photon fluence rates (F_{500}/F_{λ}) versus wavelength (λ) in nanometers at the point of choice neutralization should resemble the absorption spectra of the photoreceptor (*33*). As described above, the photon fluence rate at 500 nm was kept constant (1.59×10^{14}/s per cm^2), whereas the amount of light for other wavelengths (F_{λ}) was modulated to determine minimum light required for choice neutralization in binary assays. This obtained profile was matched with the predicted spectrum of the alpha band of an opsin with a λ_{max} of 475 nm, based on Govardovskii's template (*34*).

Extraocular photoreception and phototaxis

For determining wavelengths that affect extraocular phototaxis, planarian tail pieces (24 hours after decapitation; fig. S2B) were subjected to phototaxis assays similar to the single-input phototaxis assays. We measured the extraocular response using LEDs that showed their peak response at the following wavelengths from 365 to 625 nm. The intensity of all the light sources was kept constant at 126 (±10) $\mu W/cm^2$. To examine the dosage (light intensity) dependence of extraocular photoreception (Fig. 5B), we performed a modified phototaxis assay. Worms were placed in a petri dish 24 hours after decapitation with planarian medium and allowed to relax for ~30 min without any light or mechanical disturbance. A 1-cm light circle was made to fall on the

worm, and the time it took the worm to escape from the circle of light was calculated and plotted against the intensity of light used. For light dosage experiments with extraocular response, the light wavelengths used were 365 and 395 nm, and the light intensity was varied from ~31 to ~506 μW/cm^2. To understand the attenuation of extraocular response on the visible side of the spectrum, we performed photoavoidance experiments with 365, 385, and 405 nm wavelengths at a photon flux of 2.33 × 10^{14}/s per cm^2 and recorded the response time.

Ocular versus extraocular binary choice assays

Binary choice assays were performed using 395 and 500 nm light inputs using intact worms by maintaining constant light intensities of 126 (±10) μW/cm^2. Similarly, to study the ocular-extraocular choice over regeneration, we subjected anterior regenerates (tail-forming head) and posterior regenerates (head-forming tail) to similar binary phototactic choice assays over a period of 8 days after head amputation.

Fluorescence in situ hybridization

The heads of asexual planarians 5 to 10 mm in length were cut and processed for FISH as per the protocol described by Pearson *et al.* (*51*) with significant modifications. The reduction step after fixation was omitted, and the worms were stored in methanol after dehydration. Bleaching was performed for 2 hours using a formamide-based solution (1.2% H_2O_2, 5% formamide, and 0.5× SSC) as described by King and Newmark (*52*) after rehydration. The post-hybridization washes, antibody blocking, incubation of peroxidase-conjugated anti-digoxigenin antibody, and post–antibody incubation washes were performed as per the protocol by King and Newmark (*52*). The development of the fluorescent signal was performed using a tyramide signal amplification (TSA) reaction as per the protocol by King and Newmark (*52*). The tyramide conjugates were synthesized according to the protocol described by Hopman *et al.* (*53*) from *N*-hydroxysuccinimide esters of Alexa Fluor 647 (A2006, Thermo Fisher Scientific). The TSA reaction was followed by at least five washes of 20 min each with PBSTx (phosphate-buffered saline with 0.3% Triton X-100) before further processing or mounting with a Mowiol-based mounting medium prepared. For experiments involving immunostaining followed by FISH, the protocol mentioned below was followed.

Whole-body immunofluorescence and imaging

Confocal immunofluorescence microscopy was performed to visualize changes in the planarian nervous system over regeneration. Immunostaining of the planarian nervous system was carried out as described by Sánchez Alvarado and Newmark (*39*) with modifications using SYNORF1 (3C11, Developmental Studies Hybridoma Bank) or VC-1 [anti-arrestin (a gift from K. Agata)] as the primary antibody. Horse serum (10%) was used as the blocking solution. A donkey anti-mouse Alexa Fluor 488/555 (A-21206/A31570, Life Technologies) secondary antibody was used at dilution 1:500, with an incubation time of 90 min at room temperature. Imaging was performed on an LSM 780 Zeiss confocal microscope and analyzed using ImageJ V. 1.48 (National Institutes of Health, Bethesda) (*54*). All stereomicroscope images were taken using Olympus SZX16.

RNAi-mediated knockdown

Planarian eye opsin (Smed eye opsin) sequence was obtained from the published planarian eye transcriptome (*12*). A region of the transcript was cloned using the following primers: Smed eye_opsin, AACACTCGATGGGCTTGGG (forward) and CCCTGTGAGAGCCATAAGGG (reverse). From the cloned region, double-stranded RNA (dsRNA) was synthesized as described by Rouhana *et al.* (*55*) with modifications. Planarians were amputated as shown in fig. S2B. Three 69-nl injections with either opsin or control (green fluorescent protein) dsRNA (2 μg/μl) were made on days 1 to 3 of anterior-regenerating worms. Subsequently, these regenerates were examined for light response on days 5 to 7 after amputation. Specifically, the regenerating worms were subjected to single-input, light-dark choice using the light inputs (425, 500, and 625 nm at 63 μW/cm^2) as described earlier. DI was calculated for opsin knockdown and control worms and then plotted.

Movie recording

All behavioral movies were recorded with Point Grey camera (GS3-U3-41C6NIR-C or BFLY-PGE-20E4M-CS). Fujinon 3.8- to 13-mm Varifocal C-mount lens were attached to the camera along with an infrared long-pass filter if required. All of these were mounted on an adjustable mounting pole as shown in fig. S11. Optic fiber used for probing in movie S11 was procured from Thorlabs as a part of customized OptoLED light system. Movie S10 was recorded on an Olympus MVX10 microscope using DP71 camera.

Bioinformatic analysis

To identify opsin homologs in planarians, we used 821 opsin sequences from Porter *et al.* (*56*) as a reference data set. To make a non-redundant planarian transcriptome data set, we used CD-HIT (*57*) to cluster multiple transcriptomes (*58*–*61*). Reverse blast was performed with (evalue = 1 × 10^{-10}; coverage, 35%) 821 opsin sequences to identify homologous sequences in *S. mediterranea*. We identified 172 putative opsin-like candidates. A total of 143 of 172 transcripts that had PFAM domain PF00001.16 (opsin G protein–coupled receptor classification) were taken for further analysis. We built a hidden Markov model (HMM) for 821 opsin sequences and compared it with the 143 transcript profiles. Of 143 transcripts, 130 matched the HMM profile with evalue <1 × 10^{-10}. We used TmHMM (www.cbs.dtu.dk/services/TMHMM-2.0/) to predict transmembrane (TM) helices for 130 transcripts. We only considered transcripts with seven TM helices with optimum loop length for further analysis. Further, 66 transcripts with seven TM helices were selected. From previous reports on opsin sequences from other organisms, we know that Lys (K) residue in the seventh (last) TM helix is the amino acid residue to which retinal binds via a Schiff base linkage (*62*). This TM helix has an NPxxY(x)$_6$F sequence motif (*62*). We took the seventh (last) TM helix for 66 *S. mediterranea* transcripts along with 821 opsin sequence and performed multiple sequence alignment using MacVector. To predict the sequence motif, we used MEME (http://meme-suite.org/). Six of 66 sequences had Lys (K) residue and complete/partial (one amino acid missing/substitution) NPxxY(x)$_6$F motif conservation. We predicted tertiary structures of the six opsin sequences using homology modeling (https://swissmodel.expasy.org/). Squid opsin (2z73) was obtained as a closest hit to our modeled three-dimensional (3D) structure of six opsins. Energy-minimized 3D structure was aligned using PyMOL (https://www.pymol.org/). In addition, we obtained a root mean square deviation of 0.167 Å, suggesting high structural similarity. We did phylogenetic analysis of the identified six putative opsins from *S. mediterranea* using MEGA7 (maximum likelihood, 50 bootstraps). The obtained phylogenetic tree was visualized using TreeDyn (www.phylogeny.fr/one_task.cgi?task_type=treedyn). Seven TRP channels were identified by Inoue *et al.* (*63*) in *Dugesia japonica*. We identified the homologs of these sequences in *S. mediterranea* using

PlanMine database (http://planmine.mpi-cbg.de) (*64*). Phylogenetic analysis of seven Smed TRP channels with human and *Drosophila* TRPA1 channels was then performed using TreeDyn.

Statistical analysis

Statistical analyses were performed using a nonparametric Wilcoxon signed-rank test.

SUPPLEMENTARY MATERIALS

Supplementary material for this article is available at http://advances.sciencemag.org/cgi/content/full/3/7/e1603025/DC1

fig. S1. Planarian light sensing apparatus.
fig. S2. Planarians are aversive to light across a broad wavelength range.
fig. S3. Planarian eye opsin knockdown attenuates light sensing across the color spectrum.
fig. S4. Recovery of single-input light sensing and response during head regeneration.
fig. S5. Wavelength dependence of extraocular photoreception.
fig. S6. Extraocular response attenuates in visible light (~405 nm and longer).
fig. S7. Aggregate time taken for eye-mediated phototaxis is insensitive to light intensity.
fig. S8. Lack of wavelength discrimination in extraocular photoresponse.
fig. S9. Phylogenetic tree (maximum likelihood) of planarian opsin sequence.
fig. S10. Phylogenetic analysis of Smed TRP channels along with known UV-sensitive TRPA1 channels (human and *Drosophila*).
fig. S11. Light setup for phototaxis experiments and recording.
movie S1. Planarian worm shows wavelength discrimination.
movie S2. Planarians show robust wavelength discrimination (group response).
movie S3. Imaging Smed eye opsin expression.
movie S4. Smed eye opsin is expressed in all photoreceptor cells.
movie S5. Regenerating cephalic ganglion (day 3).
movie S6. Regenerating cephalic ganglion (day 4).
movie S7. Regenerating cephalic ganglion (day 5).
movie S8. Regenerating cephalic ganglion (day 6).
movie S9. Regenerating cephalic ganglion (day 7).
movie S10. Extraocular photoreception and phototaxis in planarians.
movie S11. Light avoidance (extraocular) response to long UV is directional.

REFERENCES AND NOTES

1. D.-E. Nilsson, Eye evolution and its functional basis. *Vis. Neurosci.* **30**, 5–20 (2013).
2. D.-E. Nilsson, The evolution of eyes and visually guided behaviour. *Philos. Trans. R. Soc. Lond. B Biol. Sci.* **364**, 2833–2847 (2009).
3. N. Randel, G. Jékely, Phototaxis and the origin of visual eyes. *Philos. Trans. R. Soc. Lond. B Biol. Sci.* **371**, 20150042 (2016).
4. D. Arendt, J. Wittbrodt, Reconstructing the eyes of Urbilateria. *Philos. Trans. R. Soc. Lond. B Biol. Sci.* **356**, 1545–1563 (2001).
5. D. Arendt, H. Hausen, G. Purschke, The 'division of labour' model of eye evolution. *Philos. Trans. R. Soc. Lond. B Biol. Sci.* **364**, 2809–2817 (2009).
6. E. Saló, R. Batistoni, chap. 2, *The Planarian Eye: A Simple and Plastic System with Great Regenerative Capacity*, in *Animal Models in Eye Research*, P. A. Tsonis, Ed. (Elsevier, 2008), pp. 15–26.
7. H. M. Brown, T. E. Ogden, The electrical response of the planarian ocellus. *J. Gen. Physiol.* **51**, 237–253 (1968).
8. K. S. Carpenter, M. Morita, J. B. Best, Ultrastructure of the photoreceptor of the planarian *Dugesia dorotocephala*. *Cell Tissue Res.* **148**, 143–158 (1974).
9. Y. Kishida, Electron microscopic studies on the planarian eye. I. Fine structures of the normal eye. *Sci. Rep. Kanazawa Univ.* **12**, 75–110 (1967).
10. T. R. Paskin, J. Jellies, J. Bacher, W. S. Beane, Planarian phototactic assay reveals differential behavioral responses based on wavelength. *PLOS ONE* **9**, e114708 (2014).
11. D. Pineda, J. Gonzalez, M. Marsal, E. Salo, Evolutionary conservation of the initial eye genetic pathway in planarians. *Belg. J. Zool.* **131**, 77–82 (2001).
12. S. W. Lapan, P. W. Reddien, Transcriptome analysis of the planarian eye identifies ovo as a specific regulator of eye regeneration. *Cell Rep.* **2**, 294–307 (2012).
13. H. B. Sarnat, M. G. Netsky, The brain of the planarian as the ancestor of the human brain. *Can. J. Neurol. Sci.* **12**, 296–302 (1985).
14. K. Agata, Y. Soejima, K. Kato, C. Kobayashi, Y. Umesono, K. Watanabe, Structure of the planarian central nervous system (CNS) revealed by neuronal cell markers. *Zoolog. Sci.* **15**, 433–440 (1998).
15. K. Tessmar-Raible, D. Arendt, Emerging systems: Between vertebrates and arthropods, the Lophotrochozoa. *Curr. Opin. Genet. Dev.* **13**, 331–340 (2003).
16. O. Simakov, T. A. Larsson, D. Arendt, Linking micro- and macro-evolution at the cell type level: A view from the lophotrochozoan *Platynereis dumerilii*. *Brief. Funct. Genomics* **12**, 430–439 (2013).
17. P. W. Reddien, A. Sánchez Alvarado, Fundamentals of planarian regeneration. *Annu. Rev. Cell Dev. Biol.* **20**, 725–757 (2004).
18. E. Saló, The power of regeneration and the stem-cell kingdom: Freshwater planarians (Platyhelminthes). *Bioessays* **28**, 546–559 (2006).
19. F. Cebrià, M. Nakazawa, K. Mineta, K. Ikeo, T. Gojobori, K. Agata, Dissecting planarian central nervous system regeneration by the expression of neural-specific genes. *Dev. Growth Differ.* **44**, 135–146 (2002).
20. T. Inoue, H. Kumamoto, K. Okamoto, Y. Umesono, M. Sakai, A. Sánchez Alvarado, K. Agata, Morphological and functional recovery of the planarian photosensing system during head regeneration. *Zoolog. Sci.* **21**, 275–283 (2004).
21. T. Takano, J. N. Pulvers, T. Inoue, H. Tarui, H. Sakamoto, K. Agata, Y. Umesono, Regeneration-dependent conditional gene knockdown (Readyknock) in planarian: Demonstration of requirement for *Djsnap-25* expression in the brain for negative phototactic behavior. *Dev. Growth Differ.* **49**, 383–394 (2007).
22. T. W. Cronin, S. Johnsen, Extraocular, non-visual, and simple photoreceptors: An introduction to the symposium. *Integr. Comp. Biol.* **56**, 758–763 (2016).
23. B. Backfisch, V. B. Veedin Rajan, R. M. Fischer, C. Lohs, E. Arboleda, K. Tessmar-Raible, F. Raible, Stable transgenesis in the marine annelid *Platynereis dumerilii* sheds new light on photoreceptor evolution. *Proc. Natl. Acad. Sci. U.S.A.* **110**, 193–198 (2013).
24. M. L. Porter, Beyond the eye: Molecular evolution of extraocular photoreception. *Integr. Comp. Biol.* **56**, 842–852 (2016).
25. D. M. Steven, The dermal light sense. *Biol. Rev. Camb. Philos. Soc.* **38**, 204–240 (1963).
26. K.-W. Yau, R. C. Hardie, Phototransduction motifs and variations. *Cell* **139**, 246–264 (2009).
27. Y. Xiang, Q. Yuan, N. Vogt, L. L. Looger, L. Y. Jan, Y. N. Jan, Light-avoidance-mediating photoreceptors tile the *Drosophila* larval body wall. *Nature* **468**, 921–926 (2010).
28. A. Ward, J. Liu, Z. Feng, X. Z. S. Xu, Light-sensitive neurons and channels mediate phototaxis in *C. elegans*. *Nat. Neurosci.* **11**, 916–922 (2008).
29. E. Pennisi, Evolution of developmental diversity. Evo-devo devotees eye ocular origins and more. *Science* **296**, 1010–1011 (2002).
30. S. Yamaguchi, C. Desplan, M. Heisenberg, Contribution of photoreceptor subtypes to spectral wavelength preference in *Drosophila*. *Proc. Natl. Acad. Sci. U.S.A.* **107**, 5634–5639 (2010).
31. H. M. Brown, H. Ito, T. E. Ogden, Spectral sensitivity of the planarian ocellus. *J. Gen. Physiol.* **51**, 255–260 (1968).
32. G. H. Parker, *The Reactions of Planarians: With and Without Eyes, to Light*, vol. 115 of *Contributions from the Zoölogical Laboratory of the Museum of Comparative Zoölogy at Harvard College* (Harvard University, 1900).
33. E. Schäfer, L. Fukshansky, W. Shropshire Jr., in *Photomorphogenesis* (Springer, 1983).
34. V. I. Govardovskii, N. Fyhrquist, T. Reuter, D. G. Kuzmin, K. Donner, In search of the visual pigment template. *Vis. Neurosci.* **17**, 509–528 (2000).
35. T. H. Goldsmith, Optimization, constraint, and history in the evolution of eyes. *Q. Rev. Biol.* **65**, 281–322 (1990).
36. A. Kelber, L. S. V. Roth, Nocturnal colour vision—Not as rare as we might think. *J. Exp. Biol.* **209**, 781–788 (2006).
37. F. Pichaud, A. Briscoe, C. Desplan, Evolution of color vision. *Curr. Opin. Neurobiol.* **9**, 622–627 (1999).
38. J. Rister, C. Desplan, The retinal mosaics of opsin expression in invertebrates and vertebrates. *Dev. Neurobiol.* **71**, 1212–1226 (2011).
39. A. Sánchez Alvarado, P. A. Newmark, Double-stranded RNA specifically disrupts gene expression during planarian regeneration. *Proc. Natl. Acad. Sci. U.S.A.* **96**, 5049–5054 (1999).
40. T. Sandmann, M. C. Vogg, S. Owlarn, M. Boutros, K. Bartscherer, The head-regeneration transcriptome of the planarian *Schmidtea mediterranea*. *Genome Biol.* **12**, R76 (2011).
41. R. A. Medved, E. F. Legner, Feeding and reproduction of the planarian, *Dugesia dorotocephala* (Woodworth), in the presence of *Culex peus* Speiser. *Environ. Entomol.* **3**, 637–641 (1974).
42. N. Randel, A. Asadulina, L. A. Bezares-Calderón, C. Verasztó, E. A. Williams, M. Conzelmann, R. Shahidi, G. Jékely, Neuronal connectome of a sensory-motor circuit for visual navigation. *eLife* **3**, e02730 (2014).
43. E. A. Kane, M. Gershow, B. Afonso, I. Larderet, M. Klein, A. R. Carter, B. L. de Bivort, S. G. Sprecher, A. D. T. Samuel, Sensorimotor structure of *Drosophila* larva phototaxis. *Proc. Natl. Acad. Sci. U.S.A.* **110**, E3868–E3877 (2013).
44. C. M. Child, Physiological isolation of parts and fission in Planaria. *Dev. Genes Evol.* **30**, 159–205 (1910).
45. N. W. Bellono, L. G. Kammel, A. L. Zimmerman, E. Oancea, UV light phototransduction activates transient receptor potential A1 ion channels in human melanocytes. *Proc. Natl. Acad. Sci. U.S.A.* **110**, 2383–2388 (2013).
46. C. González-Estévez, D. A. Felix, M. D. Smith, J. Paps, S. J. Morley, V. James, T. V. Sharp, A. A. Aboobaker, SMG-1 and mTORC1 act antagonistically to regulate response to injury and growth in planarians. *PLOS Genet.* **8**, e1002619 (2012).

47. K. G. Ross, K. C. Omuro, M. R. Taylor, R. K. Munday, A. Hubert, R. S. King, R. M. Zayas, Novel monoclonal antibodies to study tissue regeneration in planarians. *BMC Dev. Biol.* **15**, 2 (2015).
48. J. Baguñà, R. Ballester, The nervous system in planarians: Peripheral and gastrodermal plexuses, pharynx innervation, and the relationship between central nervous system structure and the acoelomate organization. *J. Morphol.* **155**, 237–252 (1978).
49. G. Purschke, D. Arendt, H. Hausen, M. C. M. Müller, Photoreceptor cells and eyes in Annelida. *Arthropod Struct. Dev.* **35**, 211–230 (2006).
50. N. J. Oviedo, C. L. Nicolas, D. S. Adams, M. Levin, Establishing and maintaining a colony of planarians. *CSH Protoc.* **2008**, pdb.prot5053 (2008).
51. B. J. Pearson, G. T. Eisenhoffer, K. A. Gurley, J. C. Rink, D. E. Miller, A. Sánchez Alvarado, Formaldehyde-based whole-mount in situ hybridization method for planarians. *Dev. Dyn.* **238**, 443–450 (2009).
52. R. S. King, P. A. Newmark, In situ hybridization protocol for enhanced detection of gene expression in the planarian *Schmidtea mediterranea*. *BMC Dev. Biol.* **13**, 8 (2013).
53. A. H. N. Hopman, F. C. S. Ramaekers, E. J. M. Speel, Rapid synthesis of biotin-, digoxigenin-, trinitrophenyl-, and fluorochrome-labeled tyramides and their application for in situ hybridization using CARD amplification. *J. Histochem. Cytochem.* **46**, 771–777 (1998).
54. J. Schindelin, I. Arganda-Carreras, E. Frise, V. Kaynig, M. Longair, T. Pietzsch, S. Preibisch, C. Rueden, S. Saalfeld, B. Schmid, J.-Y. Tinevez, D. J. White, V. Hartenstein, K. Eliceiri, P. Tomancak, A. Cardona, Fiji: An open-source platform for biological-image analysis. *Nat. Methods* **9**, 676–682 (2012).
55. L. Rouhana, J. A. Weiss, D. J. Forsthoefel, H. Lee, R. S. King, T. Inoue, N. Shibata, K. Agata, P. A. Newmark, RNA interference by feeding in vitro-synthesized double-stranded RNA to planarians: Methodology and dynamics. *Dev. Dyn.* **242**, 718–730 (2013).
56. M. L. Porter, J. R. Blasic, M. J. Bok, E. G. Cameron, T. Pringle, T. W. Cronin, P. R. Robinson, Shedding new light on opsin evolution. *Proc. Biol. Sci.* **279**, 3–14 (2012).
57. W. Li, A. Godzik, Cd-hit: A fast program for clustering and comparing large sets of protein or nucleotide sequences. *Bioinformatics* **22**, 1658–1659 (2006).
58. B. L. Cantarel, I. Korf, S. M. C. Robb, G. Parra, E. Ross, B. Moore, C. Holt, A. Sánchez Alvarado, M. Yandell, MAKER: An easy-to-use annotation pipeline designed for emerging model organism genomes. *Genome Res.* **18**, 188–196 (2008).
59. M. J. Blythe, D. Kao, S. Malla, J. Rowsell, R. Wilson, D. Evans, J. Jowett, A. Hall, V. Lemay, S. Lam, A. A. Aboobaker, A dual platform approach to transcript discovery for the planarian Schmidtea mediterranea to establish RNAseq for stem cell and regeneration biology. *PLOS ONE* **5**, e15617 (2010).
60. S.-Y. Liu, C. Selck, B. Friedrich, R. Lutz, M. Vila-Farré, A. Dahl, H. Brandl, N. Lakshmanaperumal, I. Henry, J. C. Rink, Reactivating head regrowth in a regeneration-deficient planarian species. *Nature* **500**, 81–84 (2013).
61. S. M. C. Robb, K. Gotting, E. Ross, A. Sánchez Alvarado, SmedGD 2.0: The *Schmidtea mediterranea* genome database. *Genesis* **53**, 535–546 (2015).
62. S. D'Aniello, J. Delroisse, A. Valero-Gracia, E. K. Lowe, M. Byrne, J. T. Cannon, K. M. Halanych, M. R. Elphick, J. Mallefet, S. Kaul-Strehlow, C. J. Lowe, P. Flammang, E. Ullrich-Lüter, A. Wanninger, M. I. Arnone, Opsin evolution in the Ambulacraria. *Mar. Genomics* **24** (Pt. 2), 177–183 (2015).
63. T. Inoue, T. Yamashita, K. Agata, Thermosensory signaling by TRPM is processed by brain serotonergic neurons to produce planarian thermotaxis. *J. Neurosci.* **34**, 15701–15714 (2014).
64. H. Brandl, H. Moon, M. Vila-Farré, S.-Y. Liu, I. Henry, J. C. Rink, PlanMine—A mineable resource of planarian biology and biodiversity. *Nucleic Acids Res.* **44**, D764–D773 (2016).

Acknowledgments: We thank V. Lakshmanan for his help in bioinformatics analysis. We are grateful to M. K. Mathew, M. Panicker, A. Ramesh, S. Sane, T. Mukherjee, R. Muddashetty, R. Sambasivan, S. Mayor, and U. S. Bhalla for their discussions and advice. We thank S. Ramaswamy and the Technologies for the Advancement of Science. We are also grateful to the Central Imaging and Flow Cytometry Facility, Sequencing facility, the mechanical and electronic workshops, and other facilities at the National Centre for Biological Sciences (NCBS)–Institute for Stem Cell Biology and Regenerative Medicine (inStem) campus. **Funding:** The support from inStem core funds and Department of Biotechnology (DBT), India, is gratefully acknowledged. Work in A.G. laboratory is also supported by the following grants: 102/IFD/SAN/999/2014-2015 (DBT), BT/IN/Germany–BMBF/03/AG/2015-16 (DBT), and INT/SWISS/SNSF/P-50/2015 (Department of Science and Technology). D.P. is supported by Welcome/DBT India Alliance (GrantID: 500160/Z/09/Z). N.S. is grateful to the University Grants Commission for the fellowship support. **Author contributions:** N.S. designed and performed the experiments, analyzed the data, and assisted in manuscript writing. A.J. and S.P. assisted N.S. in performing behavioral experiments and experimental setups. R.D. and A.C. performed immunostaining and assisted in imaging. R.G. helped perform choice overturning and dose dependence experiments. M.M. assisted with light setups and the experimental design. D.P. provided expertise in planarian biology, experimental design, and bioinformatic analysis. A.G. conceived the project, designed the experiments, directed the study, analyzed the data, and wrote the manuscript with contributions from the other authors. **Competing interests:** The authors declare that they have no competing interests. **Data and materials availability:** All data needed to evaluate the conclusions in the paper are present in the paper and/or the Supplementary Materials. Additional data related to this paper may be requested from the authors.

Submitted 1 December 2016
Accepted 27 June 2017
Published 28 July 2017
10.1126/sciadv.1603025

Citation: N. Shettigar, A. Joshi, R. Dalmeida, R. Gopalkrishna, A. Chakravarthy, S. Patnaik, M. Mathew, D. Palakodeti, A. Gulyani, Hierarchies in light sensing and dynamic interactions between ocular and extraocular sensory networks in a flatworm. *Sci. Adv.* **3**, e1603025 (2017).

Science Advances

Hierarchies in light sensing and dynamic interactions between ocular and extraocular sensory networks in a flatworm

Nishan Shettigar, Asawari Joshi, Rimple Dalmeida, Rohini Gopalkrishna, Anirudh Chakravarthy, Siddharth Patnaik, Manoj Mathew, Dasaradhi Palakodeti and Akash Gulyani

Sci Adv **3** (7), e1603025.
DOI: 10.1126/sciadv.1603025